

Respiratory cycle timing and fast inspiratory discharge rhythms in the adult decerebrate rat

VITALIY MARCHENKO, ANTONIO R. GRANATA, AND MORTON I. COHEN

*Department of Physiology and Biophysics, Albert Einstein
College of Medicine, Bronx, New York 10461*

Received 21 February 2002; accepted in final form 24 June 2002

Marchenko, Vitaliy, Antonio R. Granata, and Morton I. Cohen. Respiratory cycle timing and fast inspiratory discharge rhythms in the adult decerebrate rat. *Am J Physiol Regul Integr Comp Physiol* 283: R931–R940, 2002. First published June 27, 2002; 10.1152/ajpregu.00117.2002.—In supracollicular decerebrate paralyzed adult rats, neural respiration was monitored by bilateral phrenic recordings. In the study of respiratory cycle timing, the effects of vagal afferent input (lung inflation) on respiratory phase durations resembled those seen in decerebrate cats. 1) Withholding lung inflation during neural inspiration (I) produced lengthening of I phase duration by 46% (mean, $n = 11$). 2) Maintaining lung inflation during neural expiration (E) produced lengthening of E phase duration by 112% (mean, $n = 4$). In the study of fast rhythms in inspiratory discharges, phrenic nerve autospectra and bilateral (left-right) phrenic coherences in 16 rats revealed two types of fast rhythm: 1) high-frequency oscillation (HFO), which had significant coherence peaks ($n = 9$, range 106–160 Hz, mean 132 Hz); and 2) medium-frequency oscillation (MFO), which had autospectral peaks but no distinct coherence peaks ($n = 11$, range 46–96 Hz, mean 66 Hz). These rhythms resembled MFOs and HFOs in the decerebrate cat, but the modal frequency range was about twice as large. In addition, these frequency values differed markedly from the 20–40 Hz of the rhythms found in earlier studies in neonatal in vitro preparations; the difference may be due to developmental immaturity.

phrenic; vagal afferents; high-frequency oscillations; medium-frequency oscillations; spectral analysis

IN RECENT YEARS, much of the research on neurogenesis of respiratory rhythm has been performed on in vitro preparations (most commonly obtained from neonatal rats), such as the en bloc (isolated brain stem-spinal cord) preparation and the medullary slice preparation (1). To help interpret observations made in vitro, it would be useful to make comparisons with in vivo observations. Although the major portion of earlier in vivo studies had been done in the cat (3, 32, 36), a number of in vivo studies have also been done in the rat (14, 15, 34, 41–43) and therefore might furnish suitable comparisons.

The present paper deals with aspects of two broad areas of interest in both in vitro and in vivo studies: 1) the temporal structure of the overall respiratory cycle,

such as the durations of the inspiration (I) and expiration (E) phases; and 2) the short-term timing relations between different inspiratory (phrenic) neural activities, as indicated by fast rhythms in their discharges.

With respect to respiratory cycle timing, publications from one laboratory have reported the effects of lung afferent input (inflations) on respiratory cycle timing in the en bloc preparation with lungs attached: inflations delivered during the E phase produce prolongation of that phase (27), whereas inflations delivered during the I phase result in shortening of that phase (28, 29). In previous in vivo studies from our laboratory, similar procedures involving timed application of inflations have been done in the decerebrate cat (10, 11); now, in the present study, such procedures have been applied in the decerebrate rat.

With respect to fast neural rhythms during inspiration, earlier studies from this laboratory in the adult cat have shown that such rhythms are ubiquitous in I nerve and medullary I neuron discharges (5, 6, 12, 13), in which two types of rhythm were observed: high-frequency oscillations (HFOs; 50–100 Hz) and medium-frequency oscillations (MFOs; 10–50 Hz).

Subsequently, several studies in in vitro preparations (4, 22, 35, 37) have reported the existence of 20- to 40-Hz rhythms in I discharges, although only two of those studies (22, 37) used spectral coherence analysis.

Only a limited number of rat in vivo studies have reported fast rhythms during I. Oscillations in the range 120–140 Hz were observed in cross-correlations between 1) medullary I neurons and spinal motoneurons (38) and 2) pairs of medullary I neurons (39, 40); but no detailed analysis of such oscillations was done. In two other studies (23, 24), autospectral and coherence analysis was applied to I nerve discharges in anesthetized rats. Autospectral frequency peaks, mainly in the range 20–40 Hz, were found, but significant coherence peaks at these or higher frequencies between different nerve activities were rare. This situation might have been due to anesthesia, which is known to weaken or abolish fast I rhythms (9, 20). Therefore, we initiated a project to study these rhythms in decerebrate unanesthetized rats.

Address for reprint requests and other correspondence: M. I. Cohen, Dept. of Physiology and Biophysics, Albert Einstein College of Medicine, Bronx, NY 10461 (E-mail: mcohen@aecom.yu.edu).

The costs of publication of this article were defrayed in part by the payment of page charges. The article must therefore be hereby marked “advertisement” in accordance with 18 U.S.C. Section 1734 solely to indicate this fact.

The general aim of this study was to compare the two major aspects of I neural activities in 1) rat in vivo vs. in vitro and 2) rat vs. cat in vivo preparations. In phrenic recordings from decerebrate unanesthetized rats, two major types of observation were made. 1) Lung inflation inputs (inflations) were used to produce reduction of I phase duration or increase of E phase duration; these effects were similar to those previously found in the cat. 2) Autospectral and coherence analysis, applied to bilateral phrenic recordings, showed the existence of two types of rhythm (MFOs and HFOs) analogous to those found in the cat, but with spectral frequency values approximately twice those of the respective rhythms in the cat. A preliminary report has been presented as an abstract (25).

METHODS

Preparation

Experiments were done on adult male Sprague-Dawley rats (weight range 250–350 g) that had been decerebrated at the rostral supracollicular level (41). Anesthesia was induced and surgery was performed under 2–4% halothane or isoflurane. After implantation of tracheal, venous (saphenous), and arterial (femoral) cannulas, the animal was mounted in the prone position in a headholder. The frontoparietal bone overlaying the forebrain was removed, the brain stem was transected by spatula at the rostral border of the superior colliculus, and all neural tissue rostral to the transection was removed by suction. Bleeding was controlled by application of Gelfoam pledgets soaked with thrombin solution. Thereafter, the headholder was rotated by 180°, placing the animal in the supine position, and both phrenic nerves were dissected, desheathed, and sectioned.

After completion of surgery and removal of anesthetic inhalation, the animals were paralyzed by continuous intravenous infusion of *d*-tubocurarine chloride ($3 \text{ mg} \cdot \text{kg}^{-1} \cdot \text{h}^{-1}$) and ventilated with $\text{CO}_2\text{-O}_2$ mixtures by either a fixed-rate ventilator or a cycle-triggered pump. End-tidal CO_2 was monitored by an infrared analyzer and maintained at 4–5% by adjustment of ventilation parameters. Arterial pressure was kept at >90 mmHg systolic by infusion of 0.9% saline containing 5% glucose ($5 \text{ ml} \cdot \text{kg}^{-1} \cdot \text{h}^{-1}$). Rectal temperature was maintained at 37–39° by use of a feedback-controlled heating system (CWE). A bilateral pneumothorax was performed, and to prevent lung collapse an expiratory load of 1–2 cmH_2O was attached to the exhalation port of the ventilator system. Recordings were not started until ~2 h after completion of surgery.

Recording

With the rat in the supine position, the phrenic nerves were placed on bipolar electrodes and were immersed in a mineral oil pool formed by skin flaps. Monophasic recordings (preamplifier bandwidth 0.8–5,000 Hz) of efferent activity were obtained after crushing the central end of each nerve. A leaky integrated signal was obtained from the original phrenic signal by half-wave rectification and low-pass filtering (time constant 100 ms). By means of a special circuit (8), the integrated signal was used to derive pulses marking the onset of the I and E phases.

All signals were recorded by an analog-to-digital converter system (RC Electronics) into the hard disk of a PC at sampling rates of 2,500 or 5,000 Hz (0.4- or 0.2-ms bin duration,

respectively). Recorded signals were nerve discharges, I and E pulses, arterial blood pressure, and intratracheal pressure.

Inflation Tests

To ascertain the influence of lung afferents, inflation tests were performed in animals having intact vagi and ventilated with the cycle-triggered pump system. In this system (17, 18), the I and E pulses are used to inflate the lungs during the time of phrenic discharge, thus preserving the normal phase relation between phrenic efferent and vagal afferent activities. Two types of test were applied: 1) no I inflation (10), in which inflation is not delivered during one I phase and 2) maintained E inflation (11), in which the lungs are not allowed to deflate at the end of the I phase and are kept inflated until the end of the E phase.

Data Analysis

Cycle-triggered histograms (CTHs) were obtained by ensemble averaging ($n > 15$) of phrenic nerve activities, using the I or E pulses as triggers. Before averaging, the nerve signal was subjected to high-pass filtering (40 Hz, 3-db cut-off) followed by half-wave rectification, and the potentials in the original 0.4- or 0.2-ms bins were then summed into bins of 40- or 20-ms duration. The value in each bin thus represents the integral of activity during that bin.

Spectral Analysis

The standard fast Fourier transform (2) was used to derive the autospectra of phrenic activities and the coherences of left vs. right phrenic activities. The data processing methods have previously been described in detail (5) and are now briefly summarized. The signals were processed in 2-ms bins, the data value in each bin being derived by summing the values in the original 0.4- or 0.2-ms sampling bins. This procedure acted as a low-pass filter with effective sampling rate of 500 Hz. The time windows for the data were obtained from an ensemble of I phases ($n = 20$ at least); each started at the onset of the I phase and ended at a time corresponding to the end of the shortest I phase in the sample. The purpose of this procedure was to obtain data windows of equal length.

For each data window, the autospectra and the cross-spectra (real and imaginary parts) were computed; the final spectra were obtained as averages over the ensemble and were used to compute the coherence function. Autospectral values are presented here as relative power, i.e., the value for each frequency bin is the fraction of the total energy that is present at that frequency. The coherence value is a measure of the linear correlation between two signals at a given frequency and can range from 0 to 1.0, with a value of zero indicating no correlation and a value of 1.0 indicating perfect correlation. To evaluate the statistical significance of coherence estimates, the upper 95% confidence value, which depends on the number of windows in the ensemble, was computed (21, 33). Coherence values above that value were considered to be significantly different from zero at the 95% confidence level ($P < 0.05$). The 95% confidence value is indicated as a horizontal line in the plot of the coherence function.

RESULTS

Recordings of bilateral phrenic nerve discharges were made in 16 male Sprague-Dawley adult rats that had been decerebrated at the supracollicular level and that were maintained under neuromuscular block

without general anesthesia. As seen in CTHs (Fig. 1), the overall phrenic discharge pattern was augmenting.

Effects of Vagal Afferent Input on Phase Durations

The effects of vagal afferents on respiratory cycle timing were studied by the imposition of changes in lung inflation in animals that were ventilated with a cycle-triggered pump system, where in the control state lung inflation was delivered during the neural I phase (time of phrenic discharge). Two types of inflation test were applied, as shown in the examples of Fig. 1.

No-inflation test. In this test, the influence of vagal input on I duration is tested by withholding inflation during the I phase. In the example of Fig. 1A (which shows the average of 22 tests in 1 preparation), this procedure produced a lengthening of I phase duration by 24% (from 297 to 369 ms). For the sample of 11 preparations where this test was applied, the mean

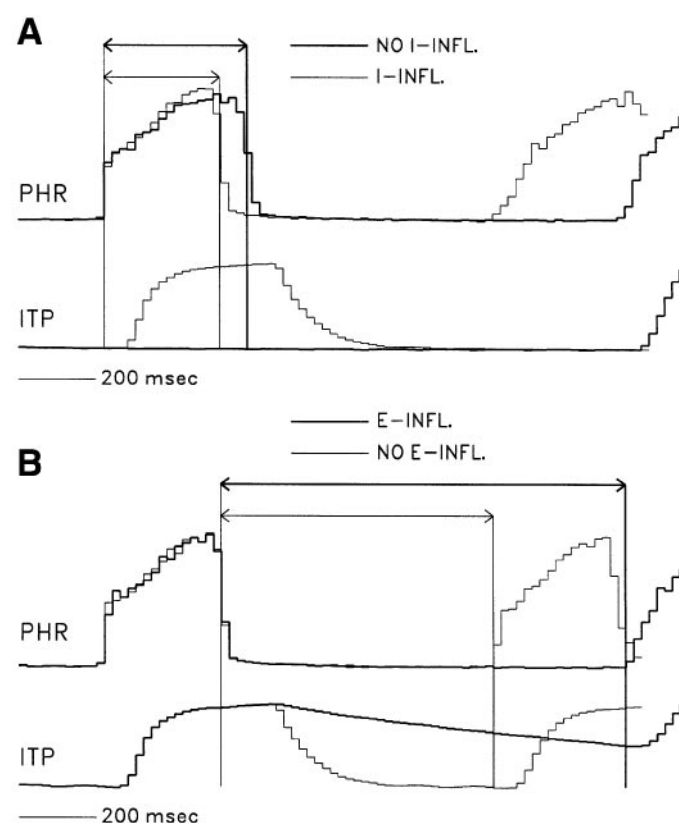


Fig. 1. Cycle-triggered histograms (CTHs; 20-ms bins) showing effects of 2 types of lung inflation test on respiratory phase duration and on phrenic (Phr) discharge. Inflation is indicated by intratracheal pressure (ITP). A: no-inflation: withholding of inflation during an inspiration (I) phase. CTHs triggered by I pulses ($n = 22$). Control cycles (thin lines): I-INFL, inflation delivered during I. Test cycles (thick lines): NO I-INFL, inflation not delivered during I. Horizontal arrowed lines indicate mean durations of control and test I phases. B: maintained expiration (E) inflation: maintenance of the I phase inflation during the subsequent E phase. CTHs triggered by E pulses ($n = 22$). Control cycles (thin lines): NO E-INFL, inflation not maintained during E. Test cycles (thick lines): E-INFL, inflation maintained during E. Horizontal arrowed lines indicate mean durations of control and test E phases.

Table 1. Effects of withholding lung inflation during I on I phase durations

	Duration, ms		Test/Control
	Control	Test	
Mean	289	405	1.46
SD	± 74	± 112	± 0.53
Min	202	276	1.09
Max	473	633	2.95

Control, inflation during inspiration (I) phase; test, no inflation during I phase; Min, minimum; Max, maximum; $n = 11$ rats.

increase of I duration was 46% (Table 1), a highly significant difference ($P < 0.01$).

Maintained inflation test. In this test, the influence of vagal input on E duration is tested by maintaining the I phase inflation during the subsequent E phase, with the inflation being released at the onset of the next I phase. In the example of Fig. 1B (which shows the average of 22 tests in the same rat as used for Fig. 1A), this procedure produced a lengthening of E phase duration by 49% (from 700 to 1,040 ms). For the sample of four preparations where this test was applied, the mean increase of E duration was 112% (Table 2), a highly significant difference ($P < 0.01$).

Fast Rhythms in Inspiratory Discharges

The properties of fast rhythms in phrenic discharges were studied by application of spectral (autospectral and coherence) analysis to bilateral phrenic recordings in 16 adult supracollicular decerebrate male Sprague-Dawley rats.

Patterns of rhythmicity in bilateral (left and right) phrenic discharges during one I phase are shown in the reconstituted digitized data of Fig. 2. The rhythms occurring during the early part of I (Fig. 2A) vs. the later part of I (Fig. 2B) are shown in 80-ms windows on a faster time base in the bottom panels of Fig. 2. The traces from early I (Fig. 2A) show a prominent bilateral rhythm with oscillation period of ~ 7 ms, whereas the traces from late I show no clear rhythmicity.

The rhythms apparent in Fig. 2 were quantified by spectral analysis as shown in Fig. 3, where the spectral distributions for both left and right phrenics are compared between the first half of I (Fig. 3A) and the second half of I (Fig. 3B). In the first half, both phrenics had a prominent autospectral peak at ~ 143 Hz; moreover, this rhythm was correlated between left and right

Table 2. Effects of maintained lung inflation during E on E phase durations

	Duration, ms		Test/Control
	Control	Test	
Mean	587	1,205	2.12
SD	± 114	± 137	± 0.46
Min	466	1,081	1.51
Max	717	1,340	2.56

Control, no inflation during expiration (E) phase; Test, maintained inflation during E phase; $n = 4$ rats.

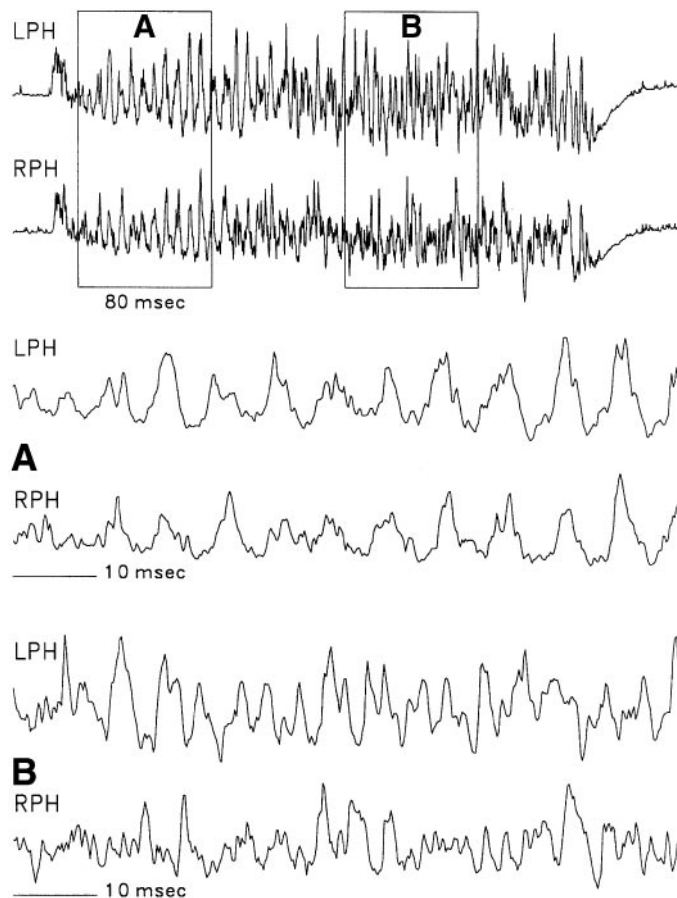


Fig. 2. Left (LPH) and right phrenic (RPH) discharges showing fast rhythmic patterns during one I phase (in which inflation was delivered). Digitized data reconstituted using digital filtering (20–200 Hz) for the purpose of smoothing the display. *Top* set of traces: display of the whole I phase. Rectangles indicate portions used for expanded displays in the *bottom* sets of traces (A: 15–95 ms from I onset; B: 175–255 ms from I onset). The traces from early I (A) show a prominent oscillation (period ~ 7 ms) that is synchronized between the 2 phrenics, while the traces from later I (B) show no clear rhythms or synchronization.

phrenics, as indicated by a prominent coherence peak (peak amplitude = 0.67). In the second half, this component was drastically reduced, the peak being only slightly above the flat level in the coherence distribution; moreover, the frequency value of the peak was reduced to ~ 133 Hz. Thus the fast rhythmic component in Fig. 3 had properties similar to the HFO previously recorded in I discharges of the cat (5–7, 9, 13) and may therefore be designated as HFO. The crucial property of HFOs was the presence of strong coherence peaks common to different I nerve signals.

In spectral analyses in the cat, another frequency component had been found (13), designated as MFO. This component had an autospectral peak that had lower values of frequency and amplitude than those of the accompanying HFO; but the crucial property of MFOs was the absence or dispersed character of distinct coherence peaks for the left-right phrenic signal pairs.

In the sample of 16 rat preparations, fast rhythms in phrenic discharges were classified as MFO or HFO on the basis of the absence or presence, respectively, of distinct peaks in the left-right phrenic coherence spectra. The distribution of peak MFO and HFO frequency values is shown in Fig. 4. In nine rats, HFO spectral peaks were present, with mean coherence peak frequency of 132 Hz and frequency range of 106–160 Hz. These were identified as HFOs by the presence of distinct left-right phrenic coherence peaks, with mean amplitude value of 0.42 and amplitude range of 0.29–0.73. In 11 rats, MFO spectral peaks were present, with mean autospectral frequency of 66 Hz and frequency range of 46–96 Hz. For 10/11 of these, there was no distinct coherence peak at the autospectral peak frequency, a feature that identified these rhythms as MFOs; in the remaining case, there was an MFO coherence peak of lower frequency and amplitude than the accompanying HFO peak. In four preparations, both MFO and HFO were present, as indicated by vertical lines in Fig. 4.

The spectral analysis for a preparation where only MFOs were present is shown in Fig. 5. It can be seen that in the first half (Fig. 5A) and second half (Fig. 5B) of the I phase there are prominent autospectral peaks for both phrenics, with higher-frequency values for the second than for the first half (88 vs. 69 Hz, respectively). However, the coherence spectra for both halves show no distinct peaks, and therefore these autospectral components are classified as MFOs.

The spectral analysis for a preparation where both MFOs and HFOs were present is shown in Fig. 6. It can be seen that in each half of the I phase there is a prominent pair of autospectral peaks for both phrenics. However, for the first peak (at lower frequency) of each pair, there is no distinct left-right phrenic coherence peak, whereas for the second peak (at higher frequency) of the pair there is a distinct coherence peak. Therefore, the lower-frequency member of each pair is designated as MFO, with peak autospectral frequency at 51 Hz for the first half and 55 Hz for the second half; and the higher-frequency member of each pair is designated as HFO, with peak coherence frequency at 117 Hz for the first half and 107 Hz for the second half.

In the examples of Figs. 3, 5, and 6, the frequency values of both MFO and HFO spectral peaks differ between the two halves of the I phase: the MFO frequency is greater in the second half, whereas the HFO frequency is smaller in the second half. This difference holds for the population samples of the two types of rhythmic component, as shown in Fig. 7, where the percent change of spectral frequency from first to second half is plotted for each preparation, together with the sample means and SEs. In Fig. 7A, the distribution of percent changes for MFO occurrences ($n = 11$) is shown (mean +24.9%, range +6.0 to +48.0%). In Fig. 7B, the distribution of percent changes for HFO occurrences ($n = 7$) is shown (mean -9.8%, range -4.8 to -15.4%). These differences with time during the I phase are similar to those found in the cat (5, 13).

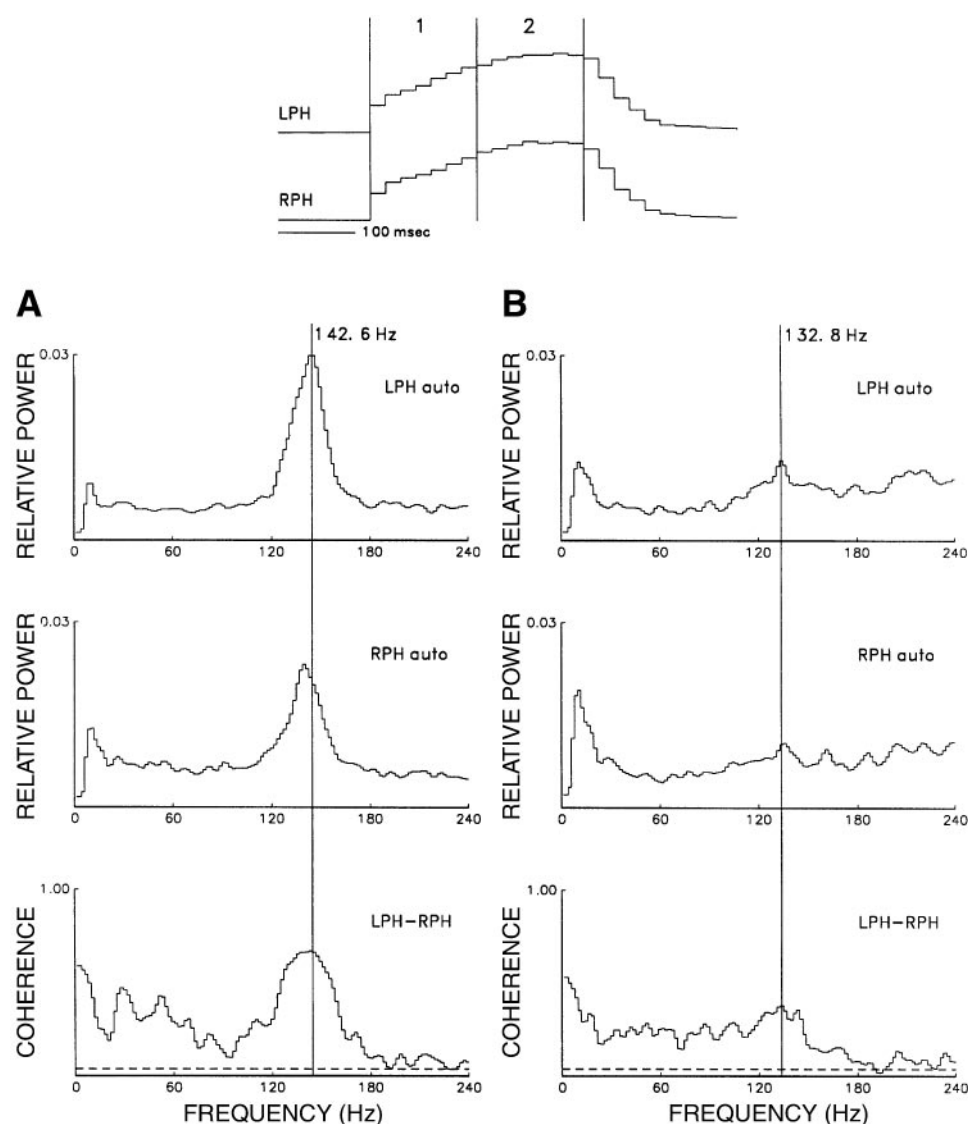


Fig. 3. Spectral analysis of bilateral phrenic (LPH and RPH) discharges in a rat (no. 15 in Fig. 4) that showed high-frequency oscillation (HFO) but not medium-frequency oscillation (MFO). This preparation furnished the data shown in Fig. 2. *Top*: CTHs (20-ms bins) derived from 84 I phases. The vertical lines show the division of each phase into 2 windows: 1, first half of I (0–140 ms from I onset); 2, second half of I (140–280 ms from I onset). *Bottom*: spectra (bin size 1.95 Hz) for activity during first half of I (A) and second half of I (B): vertically, autospectra of LPH, of RPH, and coherence between left and right phrenics (LPH-RPH). Note that for the first half there are prominent autospectral peaks and a prominent coherence peak (value of 0.67) at the common frequency of 142.6 Hz; but for the second half there are only small distinct peaks at a common frequency (132.8 Hz), with peak coherence value of 0.38. In the coherence plots, the dotted horizontal line indicates the 95% confidence limit ($P < 0.05$).

DISCUSSION

Respiratory Phase Timing

The effects of lung inflation tests on respiratory phase timing in the decerebrate rat were qualitatively similar to effects seen in earlier studies in the decerebrate cat (10, 11).

I phase duration. In the rat, lung afferent input during I shortens I phase duration, as shown by the effect of withholding lung inflation, which produced a mean increase of duration by 46% (Table 1). In the decerebrate cat, this procedure produced a mean increase of 66% (10). This qualitatively similar change occurred even though control (inflation) I duration in the rat was about half that in the cat (means 289 vs. 590 ms, respectively).

E phase duration. In the rat, lung afferent input during E lengthens E phase duration, as shown by the effect of maintained lung inflation, which produced a doubling of duration (112% increase, Table 2). In the decerebrate cat, this procedure produced a mean in-

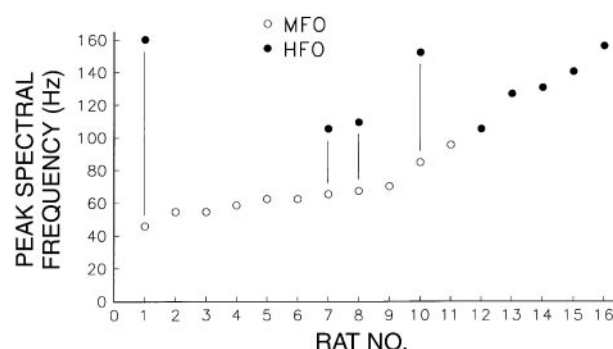


Fig. 4. Distribution of values of peak spectral frequencies in phrenic discharges of 16 rats. For each rat, windows used for computation have durations equal to that of the shortest I phase in the sample. MFOs: $n = 11$ rats. For each case, the ordinate is the mean of the autospectral peak frequency values for left and right phrenics. Values are arranged on the abscissa by increasing peak autospectral frequency value (range 46–96 Hz). HFOs: $n = 9$ rats (range 106–160 Hz). For each case, the ordinate is the left-right peak coherence frequency value. Cases with no accompanying MFOs ($n = 5$; rats 12–16) are arranged on the abscissa by increasing peak coherence frequency value; cases with accompanying MFOs ($n = 4$) are indicated by vertical lines connecting the MFO and HFO peak frequency values.

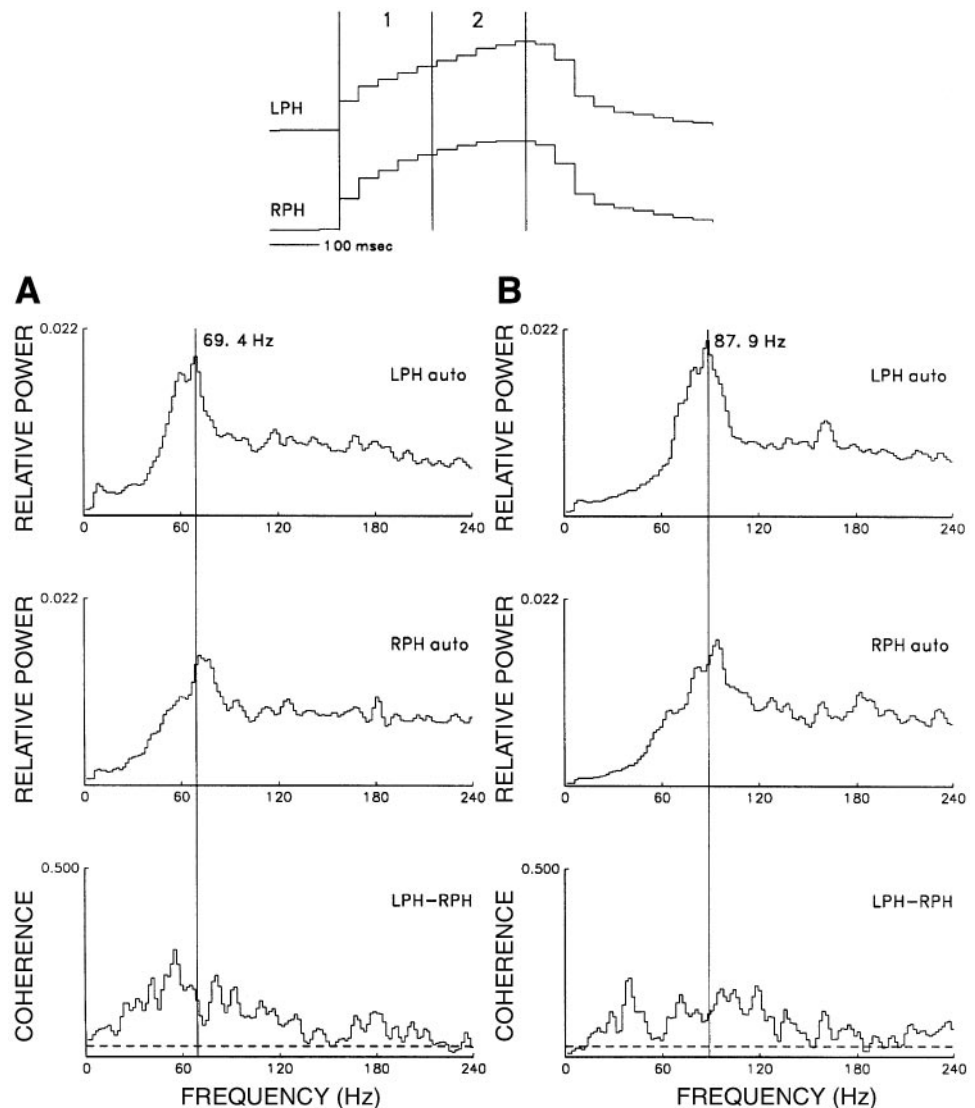


Fig. 5. Spectral analysis of bilateral phrenic discharges in a rat (no. 5 in Fig. 4) that showed MFO but not HFO. *Top*: CTHs (40-ms bins) derived from 108 I phases. The vertical lines show the division of each phase into two windows: 1, first half of I (0–190 ms from I onset); 2, second half of I (190–380 ms from I onset). *Bottom*: format similar to that of Fig. 3. Note that for both halves there are prominent autospectral peaks but there is no distinct left-right coherence peak and that the autospectral peak for the second half of I (B) has a higher frequency value than that for the first half (A) (87.9 vs. 69.4 Hz, respectively).

crease of 109% (11). This similar change occurred even though control (no inflation) E duration in the rat was about half that in the cat (means 587 vs. 1,210 ms, respectively). Thus the magnitude of the two types of Breuer-Hering reflex seemed to be scaled in relation to the spontaneous phase durations characteristic of each species.

The effects of lung inflation inputs on phase durations in *in vitro* neonatal rat preparations (27–29) were in the same direction as those found *in vivo*, thus indicating that the Breuer-Hering reflexes are well developed at birth.

Fast Rhythms in Inspiratory Discharges

By the use of autospectral and coherence analyses, the frequency content of the fast rhythms in phrenic discharges of the decerebrate rat was ascertained. The spectral frequencies fell into two ranges that, by analogy to similar rhythms in the cat (13), were designated as MFOs and HFOs.

At this point, it is necessary to discuss and justify the criteria used for classification of rhythms into the two categories. In the experiments on the decerebrate cat that led to the characterization of MFOs and HFOs (13), the majority of the animals had two peaks in the phrenic autospectra, with frequency values in the MFO range and in the HFO range, respectively. In addition, in each cat the bilateral (left-right) phrenic coherence had a well-defined peak in the HFO range, whereas in the MFO range the coherence had either no distinct peak or a broadly dispersed peak of lower amplitude than the HFO peak. Therefore, the MFO and HFO rhythms were distinguished on the basis of two criteria: frequency value and coherence value.

However, in the rat preparations (Fig. 4), only 4/16 had dual peaks (example in Fig. 6), so that where only one peak was present it would be problematic to identify a rhythm on the basis of autospectral frequency value alone. Therefore, the rhythms were categorized

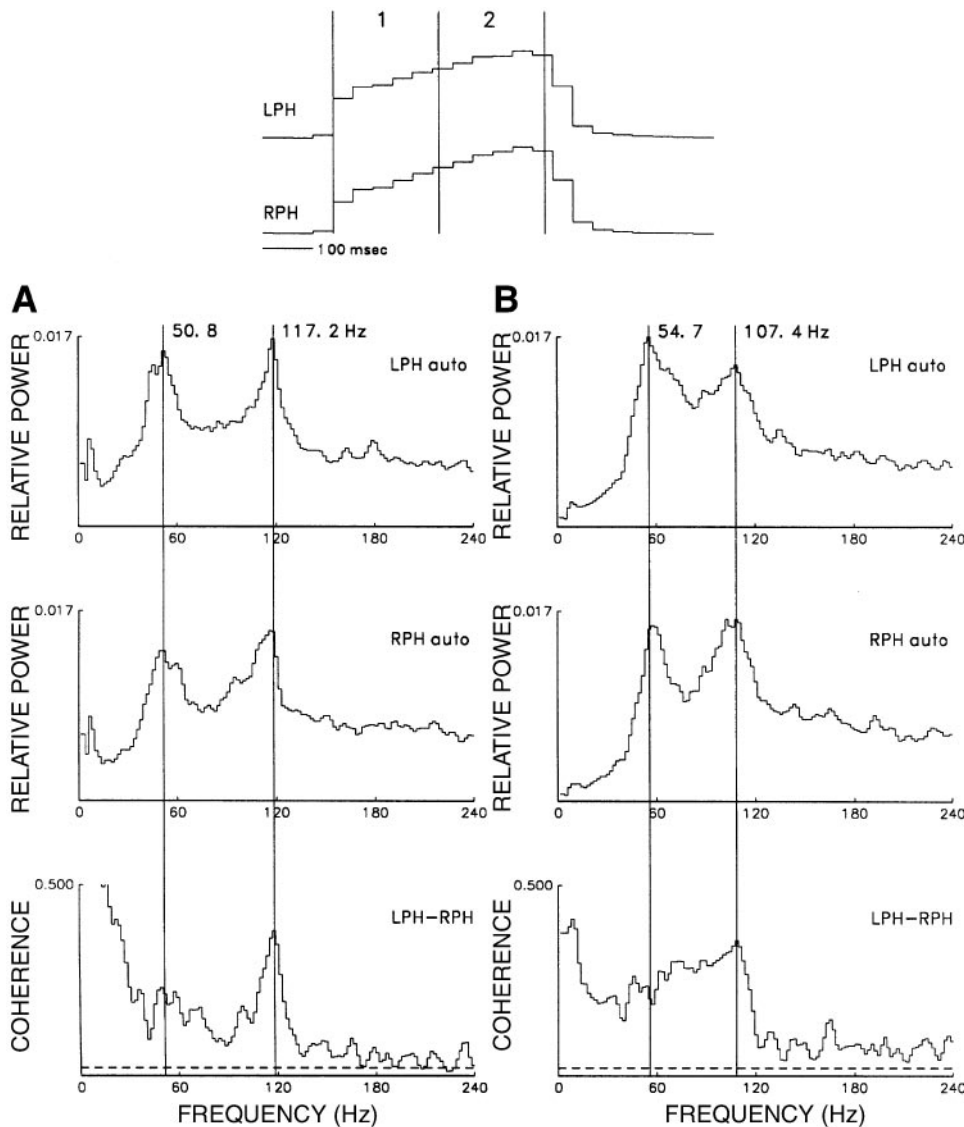


Fig. 6. Spectral analysis of bilateral phrenic discharges in a rat (no. 8 in Fig. 4) that showed both HFO and MFO. *Top*: CTHs (40-ms bins) derived from 147 I phases. The vertical lines show the division of each phase into two windows: 1, first half of I (0–212 ms from I onset); 2, second half of I (212–424 ms from I onset). *Bottom*: format similar to that of Fig. 3. Note that for each half of I there are 2 prominent autospectral peaks, designated as MFO and HFO, respectively [for the first half (A), at 50.8 and 117.2 Hz; for the second half (B), at 54.7 and 107.4 Hz]; but only the HFO component has a distinct left-right coherence peak (value of 0.31 for the first half).

only on the basis of the bilateral phrenic coherence: presence of a distinct coherence peak led to designation as HFO, whereas absence of a coherence peak (together with presence of an autospectral peak) led to designation as MFO.

After categorization by coherence, the frequency value of the peak was considered as a dependent variable, and the relationship to the independent variable of rhythm type was ascertained, as shown in the distribution of Fig. 4. It can be seen that there is no overlap of spectral frequency value between the two independently characterized rhythm types. Thus the categorization by coherence was capable of separating two distinct sample populations having different peak spectral frequency values.

Comparison of Fast Rhythms in Rat vs. Cat

Comparisons of properties of fast rhythms between the two species, rat in this study and cat in the earlier study (13), are shown in Table 3. The rhythms in the

two species are qualitatively similar with respect to 1) occurrence of two types of rhythm, and 2) dependence of frequency properties on time during the I phase. However, there are quantitative differences with respect to 1) incidence of the rhythms, 2) frequency values of the rhythms, and 3) temporal dependence of frequency values.

Incidence of rhythms. The incidence of HFOs is lower in the rat than in the cat. For the samples of Table 3, HFOs were found in 9/16 rats and in 13/13 cats; and in a host of other experiments over the years, HFOs were absent only in 5–10% of decerebrate cats. This lower incidence might be due to differences in physiological state between preparations, such as 1) difference in decerebration level (supracollicular for rat vs. midcollicular for cat), and 2) differences in chemosensitivity. A more fundamental difference might be in degree of ipsilateral vs. contralateral connectivity in the medullary rhythm generator or in bulbospinal projections. This hypothesis is consistent with the observation that

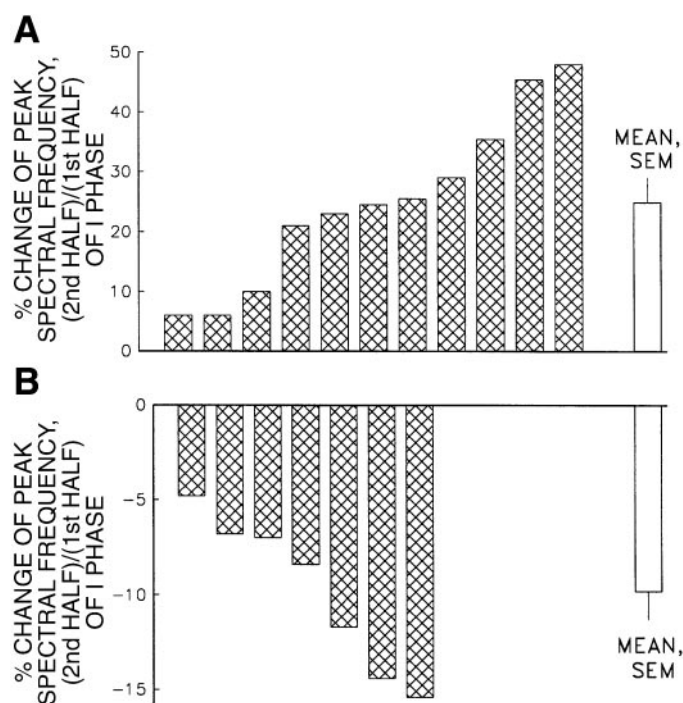


Fig. 7. Change of peak spectral frequencies between the first and second halves of the I phase for MFO (A) and HFO (B). Hatched bars, individual cases; open bars, means; vertical line, SE. A: MFO occurrences ($n = 11$ cases), with mean frequency value in the second half increased by 24.9% over the first half; range of increase, 6.0–48.0%. B: HFO occurrences ($n = 7$ cases), with mean frequency value in the second half decreased by 9.8% over the first half; range of decrease, 4.8–15.4%. (Two additional HFO cases where no distinct peak remained in the second half were excluded from the calculation.) Note that ordinate scale differs between A and B.

in the rat it is easier to produce bilaterally independent rhythms of the overall respiratory cycle (30).

Frequency values. The two species are similar in having a bimodal distribution of peak frequency values (MFO vs. HFO ranges). However, the modal frequency values for each range were about several (2–3) times as high in the rat as in the cat. For the samples of Table 3, these were 1) MFOs, 46–96 Hz in rat vs. 17–33 Hz in cat, and 2) HFOs, 106–160 Hz in rat vs. 45–92 Hz in cat. Moreover, the HFO coherence values in the rat were lower than in the cat (means of 0.42 and 0.68, respectively).

Temporal dependence of frequency. The direction of the change of peak spectral frequency with time in the I phase (ratio of second half/first half) is similar between rat and cat for each rhythm type (MFO has a larger ratio and HFO has a smaller ratio), but the magnitude differs between species. For MFOs, the frequency is higher in the second half, but to a greater extent in cat than rat (ratio 1.57 vs. 1.25, respectively). For HFOs, the frequency is moderately lower in the second half, but to a greater extent in rat than cat (ratio 0.90 vs. 0.96, respectively).

These observations indicate that, although the basic mechanisms of fast rhythm generation may be similar between the two species, the time scales of the neural interactions differ. As suggested in earlier publications

(5, 7, 12), the temporal pattern of MFOs during I arises from the augmenting pattern of firing rate of motoneurons and premotor neurons as I progresses, leading to higher spectral frequencies in later portions of I. The lesser degree of peak frequency increase in rat than in cat may be due to a gradual reduction of augmentation rate as I progresses (as indicated by reduction of slope in the phrenic CTHs shown in Figs. 1, 3, 5, and 6). The explanation for the temporal pattern of HFOs as I progresses would seem to be more complex: the reduced degree of rhythmicity (amplitude and spectral frequency) in late I might be due to occlusion, relative refractoriness, or inhibition of discharge in I neurons of the generating network.

A clue to the origin of the higher HFO spectral frequency value in the rat than in the cat (Table 3, 106–160 vs. 45–92 Hz, respectively) may be provided by the observation (40) that in the rat many medullary I neurons of both the dorsal and ventral respiratory groups have very high preferred discharge frequencies (>200/s), a feature that seems to be less common in cat medullary I neurons (6). These higher discharge rates may contribute to the high HFO spectral frequency and also to the moderate degree of reduction in late I. The further exploration of this hypothesis awaits complete statistical analysis of medullary I neuron firing properties in both species.

The observation that spectral frequency values for I discharges in the rat are several times higher than these values in the cat, together with the observation that in the rat the I and E durations are about half those in the cat, suggests that the operations of the respiratory pattern generator are scaled in relation to mechanical ventilatory parameters associated with metabolic rates and surface-volume ratios. Such a scaling relation was suggested in an early paper by Gesell and Atkinson (19) that compared motor unit firing patterns in several species and indicated that across species the number of spikes per inspiratory phase was

Table 3. Comparison of HFO and MFO properties between cat and rat

	HFO		MFO	
	Cat	Rat	Cat	Rat
<i>n</i>	13/13	9/16	9/13	11/16
Peak frequency, Hz				
Range	45–92	106–160	17–33	46–96
Mean	67	132	24	66
SD	± 15	± 22	± 6	± 14
Left-right coherence				
Range	0.47–0.91	0.29–0.73		
Mean	0.68	0.42		
SD	± 0.17	± 0.16		
Frequency ratio (2nd/1st half of I)				
Range	0.88–1.02	0.85–0.95	1.09–2.51	1.06–1.48
Mean	0.96	0.90	1.57	1.25
SD	± 0.03	± 0.04	± 0.43	± 0.14

High-frequency oscillation (HFO) and medium-frequency oscillation (MFO) properties for cat are from dataset used for Cohen et al. (13) and for rat are from the present study.

approximately constant. This relation arose from the combination of two tendencies: 1) spike firing frequency was larger for smaller species, and 2) inspiratory duration was shorter for smaller species. Further research on the adaptive relation between ventilatory requirements and respiratory cycle timing would be of interest.

Comparison Between In Vivo and In Vitro Preparations

In contrast to in vivo preparations, spectral analyses applied to neonatal in vitro preparations (4, 22, 35, 37) showed rhythms only in a lower frequency range (20–40 Hz), but categorization by the coherence criterion was not possible for those studies that performed only autospectral analysis. However, in two rat in vitro studies, coherences between bilateral cervical inspiratory nerves showed the existence of peaks within that range (Ref. 37, and M. I. Cohen and J. C. Smith, unpublished observations). In addition, large coherence peaks in the 30- to 40-Hz range were observed for cranial inspiratory nerve discharges in the kitten in vitro (22). Thus for those cases the coherent 20- to 40-Hz rhythms in vitro could be categorized as HFOs.

The markedly lower spectral frequency of HFOs in the neonatal in vitro preparations compared with those in the adult in vivo preparations of the present study (20–40 vs. 100–160 Hz, respectively) may have been due to low temperature or to developmental immaturity. Because increase of temperature is associated with greater frequency of HFOs (31), the lower temperatures at which in vitro preparations are kept may cause lowering of spectral frequency. A more important factor may be the development with age of neural connectivity, which would facilitate interactions between I neurons and thus promotion of HFOs. This hypothesis is supported by the observation that in the neonatal anesthetized rat, autospectral frequencies (but not coherences) in the 20- to 40-Hz range are found, with no rhythms in higher frequency ranges being found (24).

Perspectives

In recent years, there has been considerable interest in fast neural rhythms (such as tremor) that occur in a variety of systems at various levels: cortex, thalamus, brain stem, and spinal cord (16, 26). It is hoped that the study of such rhythms will provide useful information on neural interactions that produce functionally relevant outputs. The study of such rhythms in respiratory discharges, which dates back to the early years of electrophysiological recording, has become more tractable in recent years due to advances in signal processing methods (12). Furthermore, the methods of linear spectral analysis already described could be supplemented by nonlinear methods, such as bispectral and recurrence plot analysis. Thus information gathered on this system may be useful in analysis of other rhythmic systems.

A useful aspect for further study is the relation between firing properties of individual medullary neurons and the spectral properties of the fast population rhythms. Such relations could be influenced by connectivity and by intrinsic membrane properties. Comparison of such relations in different species could furnish additional insights on the mechanisms involved in the generation of these rhythms.

This research was supported by National Heart, Lung, and Blood Institute Grant HL-27300.

Present address for V. Marchenko: Dept. of Animal Biology, Univ. of Pennsylvania, Philadelphia, PA 19104.

Present address for A. R. Granata: Depts. of Psychiatry and Physiology, New York Medical College, Valhalla, NY 10595.

REFERENCES

1. **Ballanyi K, Onimaru H, and Homma K.** Respiratory network function in the isolated brain stem-spinal cord of newborn rats. *Prog Neurobiol* 59: 583–634, 1999.
2. **Bendat JS and Piersol AG.** *Random Data Analysis and Measurement Procedures*. New York: Wiley, 1986.
3. **Bianchi AL, Denavit-Saubié M, and Champagnat J.** Central control of breathing in mammals: neuronal circuitry, membrane properties, and neurotransmitters. *Physiol Rev* 75: 1–46, 1995.
4. **Bou-Flores C and Berger AJ.** Gap junctions and inhibitory synapses modulate inspiratory motoneuron synchronization. *J Neurophysiol* 85: 1543–1551, 2001.
5. **Christakos CN, Cohen MI, Barnhardt R, and Shaw CF.** Fast rhythms in phrenic motoneuron and nerve discharges. *J Neurophysiol* 66: 674–687, 1991.
6. **Christakos CN, Cohen MI, See WR, and Barnhardt R.** Fast rhythms in the discharges of medullary inspiratory neurons. *Brain Res* 463: 362–367, 1988.
7. **Christakos CN, Cohen MI, See WR, and Barnhardt R.** Changes in frequency content of inspiratory neuron and nerve activities in the course of inspiration. *Brain Res* 482: 376–380, 1989.
8. **Cohen MI.** Discharge patterns of brain-stem respiratory neurons in relation to carbon dioxide tension. *J Neurophysiol* 31: 142–165, 1968.
9. **Cohen MI.** Synchronization of discharge, spontaneous and evoked, between inspiratory neurons. *Acta Neurobiol Exp* 33: 189–218, 1973.
10. **Cohen MI and Feldman JL.** Discharge properties of dorsal medullary inspiratory neurons: relation to pulmonary afferent and phrenic efferent discharge. *J Neurophysiol* 51: 753–766, 1984.
11. **Cohen MI, Feldman JL, and Sommer D.** Caudal medullary expiratory neurone and internal intercostal nerve discharges in the cat: effects of lung inflation. *J Physiol* 368: 147–178, 1985.
12. **Cohen MI, Huang WX, See WR, Yu Q, and Christakos CN.** Fast rhythms in respiratory neural activities. In: *Neural Control of the Respiratory Muscles*, edited by Miller AD, Bianchi AL, and Bishop BP. Boca Raton, FL: CRC, 1997, p. 159–169.
13. **Cohen MI, See WR, Christakos CN, and Sica AL.** High-frequency and medium-frequency components of different inspiratory nerve discharges and their modification by various inputs. *Brain Res* 417: 148–152, 1987.
14. **Duffin J, Tian GF, and Peever JH.** Functional synaptic connections among respiratory neurons. *Respir Physiol* 122: 237–246, 2000.
15. **Ezure K, Manabe M, and Yamada H.** Distribution of medullary respiratory neurons in the rat. *Brain Res* 455: 262–270, 1988.
16. **Farmer SF.** Rhythmicity, synchronization and binding in human and primate motor systems. *J Physiol* 509: 3–14, 1998.
17. **Feldman JL, Cohen MI, and Wolotsky P.** Powerful inhibition of pontine respiratory neurons by pulmonary afferent activity. *Brain Res* 104: 341–346, 1976.

18. **Feldman JL and Gautier H.** Interaction of pulmonary afferents and pneumotaxic center in control of respiratory pattern in cats. *J Neurophysiol* 39: 31–44, 1976.
19. **Gesell R and Atkinson AK.** Comparison of motor integration in the mouse, rat, rabbit, dog and horse. *Am J Physiol* 139: 745–755, 1943.
20. **Gootman PM and Cohen MI.** Inhibitory effects on fast sympathetic rhythms. *Brain Res* 270: 134–136, 1983.
21. **Jenkins GM and Watts DG.** *Spectral Analysis and Its Applications*. Oakland, CA: Holden-Day, 1968.
22. **Kato F, Morin-Surun MP, and Denavit-Saubié M.** Coherent inspiratory oscillation of cranial nerve discharges in perfused neonatal cat brain stem in vitro. *J Physiol* 497: 539–549, 1996.
23. **Kocsis B and Gyimesi-Pelczér K.** Power spectral analysis of inspiratory nerve activity in the anesthetized rat: uncorrelated fast oscillations in different inspiratory nerves. *Brain Res* 745: 309–312, 1997.
24. **Kocsis B, Gyimesi-Pelczér K, and Vertes RP.** Medium-frequency oscillations dominate the inspiratory nerve discharge of anesthetized newborn rats. *Brain Res* 818: 180–183, 1999.
25. **Marchenko V, Granata AR, and Cohen MI.** Respiratory timing patterns and fast inspiratory rhythms in the decerebrate adult rat (Abstract). *FASEB J* 14: A643, 2000.
26. **McAuley JH and Marsden CD.** Physiological and pathological tremors and rhythmic central motor control. *Brain* 123: 1545–1567, 2000.
27. **Mellen NM and Feldman JL.** Vagal stimulation induces expiratory lengthening in the in vitro neonate rat. *J Appl Physiol* 83: 1607–1611, 1997.
28. **Mellen NM and Feldman JL.** Phasic lung inflation shortens inspiration and respiratory period in the lung-attached neonate rat brain stem spinal cord. *J Neurophysiol* 83: 3165–3168, 2000.
29. **Mellen NM and Feldman JL.** Phasic vagal sensory feedback transforms respiratory neuron activity in vitro. *J Neurosci* 21: 7363–7371, 2001.
30. **Peever JH, Tian GF, and Duffin J.** Bilaterally independent respiratory rhythms in the decerebrate rat. *Neurosci Lett* 247: 41–44, 1998.
31. **Richardson CA and Mitchell RA.** Power spectral analysis of inspiratory nerve activity in the decerebrate cat. *Brain Res* 233: 317–336, 1982.
32. **Richter DW.** Neural regulation of respiration: rhythmogenesis and afferent control. In: *Comprehensive Human Physiology*, edited by Greger R and Windhorst U. Berlin, Germany: Springer-Verlag, 1996, p. 2079–2095.
33. **Rosenberg JR, Amjad AM, Breeze P, Brillinger DR, and Halliday DM.** The Fourier approach to the identification of functional coupling between neuronal spike trains. *Prog Biophys Mol Biol* 53: 1–31, 1989.
34. **Saether K, Hilaire G, and Monteau R.** Dorsal and ventral respiratory groups of neurons in the medulla of the rat. *Brain Res* 419: 87–96, 1987.
35. **Smith JC, Greer JJ, Liu G, and Feldman JL.** Neural mechanisms generating respiratory pattern in mammalian brain stem-spinal cord in vitro. I. Spatiotemporal patterns of motor and medullary neuron activity. *J Neurophysiol* 64: 1149–1167, 1990.
36. **St. John WM.** Neurogenesis of patterns of automatic ventilatory activity. *Prog Neurobiol* 56: 97–117, 1998.
37. **Tarasiuk A and Sica AL.** Spectral features of central pattern generation in the in vitro brain stem spinal cord preparation of the newborn rat. *Brain Res Bull* 42: 105–110, 1997.
38. **Tian GF and Duffin J.** Spinal connections of ventral-group bulbospinal inspiratory neurons studied with cross-correlation in the decerebrate rat. *Exp Brain Res* 111: 178–186, 1996.
39. **Tian GF and Duffin J.** Synchronization of ventral-group, bulbospinal inspiratory neurons in the decerebrate rat. *Exp Brain Res* 117: 479–487, 1997.
40. **Tian GF and Duffin J.** The role of dorsal respiratory group neurons studied with cross-correlation in the decerebrate rat. *Exp Brain Res* 121: 29–34, 1998.
41. **Zheng Y, Barillot JC, and Bianchi AL.** Patterns of membrane potentials and distributions of the medullary respiratory neurons in the decerebrate rat. *Brain Res* 546: 261–270, 1991.
42. **Zheng Y, Barillot JC, and Bianchi AL.** Intracellular electrophysiological and morphological study of the medullary inspiratory neurons of the decerebrate rat. *Brain Res* 576: 235–244, 1992.
43. **Zheng Y, Barillot JC, and Bianchi AL.** Medullary expiratory neurons in the decerebrate rat: an intracellular study. *Brain Res* 576: 245–253, 1992.